Thermopower of a p-type $Si/Si_{1-x}Ge_x$ heterostructure

C. Possanzini,[1] R. Fletcher,[2] M. Tsaousidou,[3] P. T. Coleridge,[4] R.L. Williams,[4] Y. Feng,[4] and J. C. Maan[1]

[1]*Research Institute for Materials, High Field Magnet Laboratory, University of Nijmegen, Toernooiveld 1, 6525 ED Nijmegen, The Netherlands.*

[2]*Physics Department, Queen's University, Kingston, Ontario, Canada, K7L 3N6*

[3]*Materials Science Department, University of Patras, Patras 26 504, Greece.*

[4]*Microstructural Sciences, National Research Council, Ottawa, Canada K1A OR6.*

(Dated: July 31, 2003)

Abstract

We report thermopower measurements in zero and low magnetic fields for a p-type Si/SiGe heterostructure. The diffusion components of both the longitudinal and transverse components are well described by the Mott approach, including the quantum oscillations at low magnetic fields. The magnetic field dependence of thermopower shows that the diffusion contribution at zero field deviates from the linear temperature dependence that would be expected for a degenerate system, probably as a result of the nearby metal-insulator transition. Phonon drag also does not behave as expected. Instead of exhibiting an approximate T^6 dependence at low temperatures appropriate to screened, hole-phonon, deformation-potential scattering, an approximate T^4 dependence is observed. This is consistent with previous observations on the energy loss rates in SiGe hole systems. The experimental data on drag are in good agreement with numerical calculations by assuming either hole-phonon scattering by an unscreened deformation-potential interaction, or by assuming a screened piezoelectric plus screened deformation-potential coupling.

PACS numbers: 73.50.Lw, 73.40.Kp

I. INTRODUCTION

In general the thermopower of two-dimensional (2D) systems is now well understood. When the system is degenerate, the diffusion component, S^d, has a simple linear temperature dependence at low temperatures. Part of this reflects the entropy of the 2D gas, and another part gives information about the elastic scattering mechanisms of the electrons.[1]

At low temperatures, the phonon-drag component, S^g, has a stronger temperature dependence, the precise form of which depends on the mechanism of electron-phonon (e–p) scattering. Systems with screened, piezoelectric e-p scattering of the carriers, e.g., GaAs based structures, have been shown to give a T^4 dependence of drag,[2,3] whereas those with only screened deformation-potential (DP) scattering show a T^6 dependence.[4] In the former case, S^g dominates S^d down to temperatures of the order of 0.3 K. However, in the latter case S^g becomes small as the temperature is reduced below about 1 K and this allows one to examine the details of the diffusion component. In previous work the only system without piezoelectric scattering for which the thermopower has been studied in detail was an electron inversion layer in a Si-MOSFET which did show the expected behaviour of both diffusion and drag.[4]

One might have anticipated that SiGe hole or electron systems would behave in a similar fashion to Si-MOSFETs because they are not expected to be piezoelectrically active. However, there are no data on electron systems, and previous thermopower work on a hole system was inconclusive[5] in that the data were at relatively high temperatures (1.5-15 K) where it is difficult to distinguish the various hole-phonon (h–p) scattering mechanisms.

The e–p (or h–p) interaction can also be probed by carrier energy loss. The energy loss rate depends on the carrier–phonon *energy* relaxation time, whereas phonon-drag thermopower reflects the carrier–phonon *momentum* relaxation time.[6,7] Thus the two types of measurement provide different but complementary ways to investigate carrier–phonon scattering. Previous measurements on the energy loss rates in SiGe electron systems are in accord with expectations. They agree with calculations assuming only screened DP e–p coupling[8] (but note that the the 2D gas was actually in a Si channel in that case). However, similar work on SiGe hole systems (where the 2D hole gas resided in a $Si_{1-x}Ge_x$ well) gave loss rates inconsistent with this mechanism. Early measurements[9] were analyzed in terms of a screened, piezoelectric h–p coupling, but more recent work[10–12] leaned towards unscreened

DP coupling (these two mechanisms are difficult to distinguish because both give the same power law dependence on T at low temperatures), with a small unscreened piezoelectric term contributing at temperatures < 0.5 K. The present thermopower measurements throw new light on this problem. In the present work we find that S^g is indeed anomalous, in a way consistent with that found from energy loss measurements.

At low magnetic fields the diffusion thermopower has a semi-classical magnetic-field dependence arising from the Lorentz force on the electrons,[1] but phonon drag, like resistivity, has essentially no field dependence.[6] Landau quantization becomes significant when the spacing of the Landau levels becomes comparable to the level broadening. Both drag and diffusion components show oscillatory behavior under these conditions. Previous experimental work[13] on a system where drag was completely dominant showed that drag oscillations are in phase with oscillations in the electrical resistivity, but there is no quantitative theory as yet. Because most previous work has been done on piezoelectrically active systems where drag has been dominant down to low temperatures, diffusion has been difficult to probe. However, it has been predicted[1,14] that at relatively low fields diffusion oscillations should be independent of the electron scattering mechanisms and should exhibit a $\pi/2$ phase shift compared to drag or resistivity oscillations. This has only been clearly seen in a single 2D system, that of the electron inversion[15] layer in Si-MOSFETs which, it will be recalled has only DP coupling. Although drag is found to be anomalous in the present hole system, it turns out to be still small enough to enable us to investigate the behavior of diffusion in detail and the predicted phase difference is clearly seen.

Finally, the Si-SiGe hole system is known to exhibit a metal-insulator transition (MIT) at a Landau filling factor $\nu = 3/2$. We have observed this transition in the present sample in the diffusion thermopower but in an unexpected way.[16] Whereas the resistivity tends to infinity at $\nu = 3/2$ as $T \to 0$, the thermopower tends to zero or a very small value. The system is also known to undergo an apparent MIT at low densities in zero magnetic field. Although this latter transition is not observable in the present work, our sample is relatively close to the transition on the metallic side. It is of interest to determine if this system shows any other unusual behavior of the thermopower at zero or low magnetic fields.

II. THEORY

A. Thermopower at zero magnetic field

The present system is a 2D hole gas (2DHG) so we will write the results down in a form appropriate to this case. As far as thermopower is concerned, the main difference compared to electron systems is that the carriers act as if they have positive charge. In the limit of weak coupling between carriers and phonons, the contributions due to diffusion and drag are additive and the total thermopower S is given by $S = S^d + S^g$.

The diffusion component S^d of thermopower for degenerate 2DHGs is given by Mott's expression

$$S^d = L_\circ eT \left(\frac{\partial \ln \sigma}{\partial E} \right)_{E_F} \tag{1}$$

where e is the magnitude of the electron charge, σ is the conductivity, E is the hole energy (with E_F the Fermi energy) and $L_\circ$ is the Lorenz number $\pi^2 k_B^2/3e^2$. By invoking the conventional assumption[1] that the energy dependence of the hole relaxation time is $\tau_t \propto E^p$ we readily find

$$S^d = \frac{L_\circ eT}{E_F}(1+p) \tag{2}$$

The first term in Eq.(2), $L_\circ eT/E_F$, is the entropy per unit of charge of the 2DHG and the second term reflects the scattering mechanisms.

The phonon-drag component S^g of thermopower is due to the quasi-elastic scattering of 2D holes with wave vector $\mathbf{k} = (k_x, k_y)$ by 3D acoustic phonons of wave vector $\mathbf{Q} = (\mathbf{q}, q_z)$ in the substrate. Here we use the standard expression of S^g (e.g., see Ref. 4) modified suitably for the case of a 2DHG

$$S^g = \frac{(2m^*)^{3/2} g_v \Lambda}{16(2\pi)^3 k_B T^2 p_h e \rho_m} \sum_i \int_0^\infty \int_{-\infty}^\infty \frac{\Xi_i^2(\mathbf{Q})}{\epsilon^2(q)} C_i(\mathbf{Q}) dq\, dq_z \tag{3}$$

where m^* is the in-plane effective mass of holes, ρ_m is the mass density of Si, g_v is the valley degeneracy, p_h is the hole sheet density, Λ is the phonon mean free path and the subscript i refers to phonon polarization. $\Xi^2(\mathbf{Q})$ is the squared matrix element of the h–p interaction and $\epsilon(q)$ is the static dielectric screening function. The expression for $\epsilon(q)$ is[4,17] $1 + (Q_s/q)\xi(q)F_s(q)$ where Q_s is the screening wave vector,[17] $\xi(q)$ is unity for $q \le 2k_F$ and $1 - [1 - (2k_F/q)^2]^{1/2}$ for $q > 2k_F$ (k_F is the Fermi wave number) and $F_s(q)$ is the screening form factor that accounts for the finite thickness of the 2DHG.[4,17] Details for the factor $C(\mathbf{Q})$

are given in Ref. 4. When the energy spectrum of carriers is isotropic $\Xi(\mathbf{Q}) = \Xi_{DP}$, where Ξ_{DP} is the deformation potential constant. For materials with cubic $\bar{4}3m$ symmetry, such as GaAs, $\Xi^2(\mathbf{Q})$ accounts for both deformation potential and piezoelectric coupling. Then, $\Xi^2(\mathbf{Q}) = \Xi_{DP}^2 + [(eh_{14})^2 A_l/Q^2]$ for the longitudinal branch and $\Xi^2(\mathbf{Q}) = [(eh_{14})^2 A_t/Q^2]$ for each of the transverse branches, where h_{14} is the piezoelectric constant and A_l and A_t are the anisotropy factors given by Price.[18]

By allowing several low-T approximations in Eq. (3) (and assuming Λ is a independent of T) it can be shown that $S^g \propto T^6$ for screened DP coupling[4] and $S^g \propto T^4$ for screened piezoelectric coupling.[2,3] At low temperatures the screening dielectric function is approximated by the expression $\epsilon(q) \approx Q_s/q \propto Q_s/T$. Consequently, when screening effects are neglected (e.g., $\epsilon(q) = 1$) the temperature dependence of S^g is T^4 for DP coupling and T^2 for piezoelectric coupling.

B. Thermopower in a magnetic field

With a magnetic field, B_z, perpendicular to the plane of the 2D system there are two independent components of the diffusion thermopower. Assuming isotropy in the xy plane and taking the temperature gradient to be parallel to the x direction, the components are the longitudinal thermopower, S_{xx}, and the transverse thermopower (or Nernst-Ettingshausen coefficient), S_{yx}. At low temperatures the system is degenerate ($k_B T \ll E_F$) and elastic scattering by impurities is the dominant contribution to the momentum relaxation time τ_t. Taking into account the Lorentz force on the electrons, the diffusion components, S_{ij}^d, are expected to have the following field dependences for a 2DHG,[1]

$$\bar{S}_{xx}^d = \frac{L_\circ e T}{E_F}\left(1 + \frac{p}{1+\beta^2}\right) \tag{4}$$

$$\bar{S}_{yx}^d = \frac{L_\circ e T}{E_F}\left(\frac{p\beta}{1+\beta^2}\right) \tag{5}$$

where $\beta = \omega_c \tau_t = \mu_t B$ with μ_t the transport mobility. We have used a bar to denote that these are the non-oscillatory components. Notice that the second term in Eq. (4), which is related to the hole-impurity scattering mechanisms, disappears at high fields ($\beta \gg 1$) and $\bar{S}_{xx}^d$ is a direct measure of the entropy per unit charge in this limit. Also notice that in the present system the value of p is close to -2 at low T (details are given later) thus $\bar{S}_{xx}^d$ will change sign at fields when $\beta \sim 1$.

At low temperatures, oscillations in ρ_{ij} and S_{ij}^d begin to appear at magnetic fields for which the Landau level separation $\hbar\omega_c$ exceeds the level broadening $\sim \hbar/\tau_q$, i.e. at $\omega_c\tau_q \sim 1$, where ω_c is the cyclotron frequency and τ_q is the quantum lifetime. When the Landau levels are not completely resolved and localized states play no role, the oscillations in S_{ij}^d, say $\tilde{S}_{ij}^d$, can be evaluated using relations based on the Mott approach.[1] In this model it turns out that $\tilde{\rho}_{ij}$ and $\tilde{S}_{ij}^d$ are intimately related. The basic assumptions are that the electron scattering is elastic and that the energy dependent conductivity σ_{ij} contains terms which oscillate with electron energy due to the Landau levels. Under these conditions one can show that[1]

$$\tilde{S}_{xx}^d = \frac{\alpha}{1+\beta^2}\left(\frac{\tilde{\rho}_{xx}}{\bar{\rho}_{xx}} + \beta^2\frac{\tilde{\rho}_{yx}}{\bar{\rho}_{yx}}\right), \tag{6}$$

$$\tilde{S}_{yx}^d = \frac{\alpha\beta}{1+\beta^2}\left(\frac{\tilde{\rho}_{xx}}{\bar{\rho}_{xx}} + \frac{\tilde{\rho}_{yx}}{\bar{\rho}_{yx}}\right). \tag{7}$$

In the above equations, $\alpha = i(\pi k_B/e)[D'(rX)/D(rX)]$ where $D(X) = X/\sinh X$ is the thermal damping factor for resistivity oscillations with $X = 2\pi^2 k_B^2 T/\hbar\omega_c$, and $D'(X) = dD(X)/dX$ is the thermal damping factor for diffusion thermopower oscillations. We use the tilde to denote an oscillatory component and a bar to denote the smooth background in all quantities. These equations are to be applied to each harmonic, r, of the oscillatory parts. The factor $i = \sqrt{-1}$ indicates that the oscillations in S_{ij}^d and ρ_{ij} have a phase difference of $\pi/2$. Noting that $D'(X)$ is a negative quantity, if we write $\tilde{\rho}_{xx} \propto \cos[(2\pi rf/B) + \phi_r]$, then $\tilde{S}_{xx}^d \propto \sin[(2\pi rf/B) + \phi_r]$, where f is the frequency of the fundamental component and ϕ_r a constant phase factor of the rth harmonic. Interestingly, the phase shift is in the opposite sense for electron systems, i.e. $\tilde{S}_{xx}^d \propto -\sin[(2\pi rf/B) + \phi_r]$ in that case.

When $\beta = \omega_c\tau_t \gtrsim 1$, the thermopower oscillations are reduced in amplitude by the factor $(1+\beta^2)$ that appears in the denominators of Eqs. (6) and (7). Because the oscillations only begin to appear when $\omega_c\tau_q \sim 1$, and given that $\tau_t \geq \tau_q$, then the approximate equivalence of τ_t and τ_q that is found in the present system[19] is the most favorable case for producing the largest possible oscillations. This is in contrast to systems where low-angle electron scattering dominates and $\tau_t \gg \tau_q$, e.g. most GaAs heterostructures.

In the quantum Hall region, the diffusion oscillations are again expected to reflect the entropy of the electrons. We will not reproduce detailed theoretical results for this case since we have dealt with this aspect previously.[16] As we mentioned in Section I, the diffusion thermopower oscillations are in phase with those in the resistivity in this limit. Interestingly the same phase shift occurs in 3D systems[20] showing that the quantum Hall effect is not

required for this to happen.

A complete theory of phonon drag in a magnetic field is not yet available. Semi-classical theory[6] predicts that $\bar{S}^g_{xx}$ is independent of B, and that $\bar{S}^g_{yx} = 0$. The available evidence is in agreement with these predictions, except for S^g_{yx} in 2D systems which does not seem to be zero.[15,20]

There are no theoretical results for the quantum oscillations in S^g in low fields, but experiments where drag was dominant[13] showed that the oscillations in S^g_{xx} are in phase with those in ρ_{xx}. Thus, in principle it is possible to distinguish which mechanism is responsible for the thermopower oscillations from any phase difference between them and the resistivity oscillations; a phase difference of $\pi/2$ implies diffusion thermopower, and no phase difference means that phonon-drag oscillations are dominant. However, at high fields both the diffusion and drag oscillations are in phase with the resistivity oscillations so that an unambiguous identification is not possible by this method.

III. EXPERIMENTAL TECHNIQUES

The sample was a strained $Si/Si_{0.88}Ge_{0.12}$ heterostructure grown on a n-type substrate of Si with a 40 nm $Si_{0.88}Ge_{0.12}$ quantum well. The growth sequence and further details have been described elsewhere.[19] By applying a substrate bias, measurements at two different densities ($p_h = 1.9 \times 10^{15}\mathrm{m}^{-2}$ and 2.7×10^{15} m^{-2}) could be performed, but unless specifically noted otherwise, we will present data only for the higher density sample. At 1 K, the mobilities were 1.3 m^2/Vs and 1.5 m^2/Vs respectively and had a strong temperature dependence.[19] Using an effective mass[19] of $0.30m_e$, the Fermi temperatures are estimated to be 18 K and 25 K for the two samples. Under normal conditions we would not have anticipated such a strong mobility variation at such low temperatures. This feature has also been observed previously[21] in Si-MOSFETs and in both cases has been ascribed to the effects of a MIT at a somewhat lower density of about $\sim 1.0 \times 10^{15}$ m^{-2}.

All measurements were made in high vacuum in a ^{3}He cryostat which covered the range 0.26-4.2 K. Zero field data were obtained using dc techniques. With thermopower it was necessary to eliminate small temperature-dependent offset voltages in the signal.[22] This was done by measuring the voltage across the sample with and without establishing a temperature gradient, keeping the average temperature of the sample constant. The source and

drain contacts, separated by 2.8 mm, were used for this purpose. For the measurements in magnetic field, a standard ac lock-in technique was used[2] with a detection frequency of 4Hz. The ac signal sensitivity under these conditions was calibrated by using the dc thermopower at zero field. Sweep data were obtained for both $\pm B$ and the appropriate combinations of data were used to calculate the required coefficients. There was relatively little admixture of the coefficients.

IV. RESULTS AND DISCUSSION

In order to check the thermometry, the thermal conductivity λ of the n-type Si substrate was measured as a function of temperature. It was found that $\lambda = 1.8T^{2.75\pm0.02}$ W/mK provided an excellent fit over the whole temperature range, 0.27–4.2K. The deviation of the exponent from the expected T^3 result for boundary scattering may be due to weak phonon scattering from impurities. Using the low temperature theoretical limit[2] of λ, we estimate the mean free path of the phonons, Λ, in the substrate to be ~ 1.6 mm at 1 K, assuming longitudinal and transverse sound velocities of $v_l = 8861$ m/s and $v_t = 5331$ m/s respectively.

In the next two sections we will present our results on the thermopower in a magnetic field and at zero field. The results in a magnetic field are best considered first as they reveal information that is needed in the interpretation of the zero field data.

A. Thermopower in a magnetic field

Both the longitudinal and Hall resistivities, ρ_{xx} and ρ_{yx}, are needed in the analysis of $\tilde{S}^d_{ij}$, and examples are shown in Fig. 1. If we examine only the oscillatory components at the fundamental frequency, also shown in Fig. 1, the oscillations in ρ_{yx} are found to be accurately π out of phase with those in ρ_{xx} at low fields, as expected,[23] but there is a gradual shift in phase above about 1 T such that by 3 T the phase difference approaches $\pi/2$. This behavior has been observed previously in GaAs heterostructures and the phase shift has been ascribed to the appearance of localized states between the Landau levels[23,24] which primarily affects ρ_{yx}.

Examples of the data on S_{xx} and S_{yx} are shown in Figs. 2 and 3. As anticipated in Section II, the oscillations in S_{ij} at lower fields, which we identify with $\tilde{S}^d_{ij}$ (see below), are

superimposed on a varying non-oscillatory background due to $\bar{S}^d_{ij}$, implying $\tau_t \sim \tau_q$. Notice that $\bar{S}^d_{xx}$ changes sign from negative to positive as the field increases showing that $p < -1$ in Eq. (4). Close examination of the data also shows that the oscillations in S_{xx} and S_{yx} are in phase with each other, and that both are about $\pi/2$ out of phase with the oscillations in ρ_{xx}, these features being in agreement with Eqs. (6) and (7). The $\pi/2$ phase difference between $\tilde{\rho}_{xx}$ and $\tilde{S}_{ij}$ is particularly clear when one examines only the fundamental oscillatory components of the measured data (not shown).

Classical results[6] predict $\bar{S}^g_{yx} = 0$ and $\bar{S}^g_{xx}$ to be independent of field. Thus, in principle, one need only calculate $\bar{S}^d_{ij}(B)$ using Eqs. (4) and (5) to obtain the semi-classical backgrounds. Previous experience with a similar calculation for Si-MOSFETs[15] has shown that the best value of μ_t to describe $\bar{S}_{ij}$ is not necessarily the same as that taken from the resistivity and so this was left as a free parameter. Thus each data set on $\bar{S}_{xx}$ was fitted to Eq. (4) but with an additive constant to take into account $S^g(T)$. The relevant equation can be written $S = c + d/[1 + (\mu_t B)^2]$ where μ_t, c and d (with $d = pL_0eT/E_F$) are free parameters with $c + d$ being just the zero field value of S_{xx}.

The results on p and μ_t from this procedure are shown in Fig. 4 and Fig. 5 respectively, and both are seen to be temperature dependent. Also shown in Fig. 5 are data on μ_t taken from the zero field mobility and these are also temperature dependent. This latter dependence arises from the MIT in this system at a somewhat lower hole-density[19] which is known to have a significant effect on the temperature dependence of resistance (and hence mobility) on the metallic side of the transition to rather high densities. Within experimental error it is possible that the two sets of data on μ_t coincide as $T \to 0$, though they seem to become more divergent as T increases. The same general behaviour has also been seen in a Si-MOSFET,[15] though in that case the zero field mobility was essentially constant because the sample was well away from the MIT. The reason why S_{xx} yields a systematically lower value of μ at higher temperatures in both samples is not known.

The strong dependence of p with T that we see here was not seen in the Si-MOSFET data. At low temperatures when impurity scattering dominates, we would normally expect p (and therefore S^d/T) to be constant for a degenerate system, and this was the case for the Si-MOSFET data; for the present case we estimate the departure of S^d/T from a constant due to non-degeneracy to be less than 1% at 1 K, which is too small to be significant. Further, phonon scattering of the electrons cannot be the cause since, as we show later, it is

completely negligible compared to impurity scattering in this sample. We presume that the nearby MIT is the cause of the variations in p that we see here. The value of p depends on the electron-impurity scattering mechanisms (e.g., impurity and interface roughness scattering) and has been calculated for GaAs heterostructures and Si-MOSFETs,[25] but not yet for SiGe heterostructures. However, the fact that p depends on T clearly shows that there are underlying changes in the system with temperature which must be understood before a calculation along these lines is meaningful.

$\bar{S}^d_{ij}$ was calculated using Eqs. (6) and (7). There is no theory for $\bar{S}^g_{xx}$. However, S^g is small at low temperatures and S^g_{yx} should always be zero, so that $\bar{S}^g_{ij}$ should be small. We ignore it in the first instance and compare the measured oscillatory data only with calculations of $\tilde{S}^d_{ij}$.

The calculation of $\tilde{S}^d_{ij}$ proceeded as follows. Data on ρ_{ij} were available at nominally the same temperatures as S_{ij}. After removing most of the non-oscillatory backgrounds, ρ_{xx} and ρ_{yx} were Fourier transformed and the frequency spectra separated into sections, each containing a single harmonic component (retaining 3 harmonics at lower temperatures and 2 at higher temperatures). Taking the inverse Fourier transforms of each section then produced waveforms for the individual harmonics. Using these waveforms and Eqs. (6) and (7) the harmonic components of $\bar{S}^d_{ij}$ were calculated. The phase difference of $\pi/2$ was introduced by shifting the value of B at each point by the appropriate amount; this meant that $D(X)$ and $D'(X)$ were calculated at somewhat different fields, and in fact usually at somewhat different temperatures because the experimental ρ_{ij} and S_{ij} were usually not at exactly the same temperature. Finally the harmonics were summed and added to $\bar{S}^d_{ij}$. The results are shown in Fig. 2 and 3.

The overall agreement of experiment data on S_{xx} and the calculations for S^d_{xx} is very good, but is somewhat less so for S_{yx} and S^d_{yx}. Recalling that fits to $\bar{S}_{xx}$ were used to evaluate p and μ_t, perhaps it is not surprisingly that the calculated $\bar{S}^d_{xx}$ accurately fit the experimental data. However, if we use the values taken from the zero field S^d and resistivity, the calculated $\bar{S}^d_{ij}$ are not noticeably different over the temperature range investigated here. The same features are also observed for the available data on the low density sample (not shown) where p and μ_t were not available as a function of T. The calculations for $\bar{S}^d_{yx}$ are less convincing. With Si-MOSFETs a large, temperature-dependent, anomalous component was observed for $\bar{S}_{yx}$.[15] This does not seem to be present here, though the magnitude of

$\bar{S}_{yx}$ is not well reproduced by the present calculations perhaps suggesting that unidentified problems are present.

At low temperatures the phases of the calculated oscillations in both components are in excellent agreement with the experimental oscillations. The phase difference of $\pi/2$ between $\tilde{\rho}_{xx}$ and $\tilde{S}^d_{ij}$ is maintained reasonably accurately over the whole field range, and is particularly clear when one plots only the fundamental oscillatory components of the measured data (not shown). This implies that both $\tilde{S}^d_{xx}$ and $\tilde{S}^d_{yx}$ must be almost purely diffusion at these low temperatures, thus justifying the neglect of $\tilde{S}^g_{ij}$ initially.

In both components, the calculations predict too much harmonic content at higher fields and lower temperatures. This might be due to localized states beginning to appear between the Landau levels which would invalidate the model, and is consistent with the phase shift noticed for the oscillations in ρ_{yx} at higher fields that we noted above. The magnitudes of the calculated $\tilde{S}_{xx}$ are in reasonable agreement with the observations. This remains so up to about 3 T where the longitudinal resistivity oscillations have an amplitude close to the background value. On the other hand, the calculated magnitudes for $\tilde{S}_{yx}$ tend to be too large, by about a factor of 2 at lower temperatures and higher fields, probably again reflecting the appearance of localized states.

B. Thermopower at zero field

Thermopower data at zero field, S, are shown in Fig. 6 for the region below 1.4 K. S is negative and approximately linear in T for temperatures $\lesssim 0.6$ K; this is due to S^d. At higher temperatures the deviations from linearity in the positive direction are mainly due to S^g. The situation is complicated by the fact that p is temperature dependent in Eq. (2) so there are deviations from $S^d \propto T$, also in the positive direction. Clearly this must be taken into account in the separation of S^d and S^g, in particular at lower temperatures where S^g is small. However, the data in Fig. 4 do not provide a sufficiently accurate estimate of p, and therefore S^d, at the lowest temperatures, but they do suggest that p becomes independent of T below about 0.6 K and so we can take $S^d \propto T$ in this limit.

Using this result the measured S was fitted using an expression of the form $S = aT + bT^n$ at low temperatures, with the parameters a, b and n to be determined. The value of n was found to depend on the temperature range of fit, but was always near 4 even with the

upper temperature limit as high as 1.5 K. In addition, in both samples a has a relatively small spread of values, regardless of the upper temperature limit used; the reason for this seems to be related to the fact that S^g and the deviations from linearity of S^d (see below) have a similar temperature dependence. The best estimates of a for the higher and lower density samples are $a = -13.0$ μV/K^2 and -18.5 μV/K^2 respectively. Using Eq. (2) and the values of E_F quoted in Section III, we find the scattering parameter $p = -2.15 \pm 0.10$ in both samples. The error estimate ignores systematic uncertainties which could add another 10-15%. At about 2.2 K, p has increased to -1 and at this point S^d passes through zero and becomes positive.

Lacking a theory of p as a function of T, the data on p in Fig. 4 were fitted to the phenomenological expression

$$p = p_0 + \frac{p_1}{(1 + CT^m)} \tag{8}$$

using $p_0 + p_1 = -2.15$ (from above) with p_1, C and m being free parameters. This gave $C = 0.139$ K^{-m}, $m = 3.75$ and $p_1 = -1.49$, and this curve is shown in Fig. 4. Using this expression, S^d was calculated from Eq. (2) and the lower temperature results are shown in Fig. 6. This shows that most of the deviation of S from linearity at $T \gtrsim 0.6$ K is not caused by S^d but is in fact due to S^g. The calculated values of S^d were subtracted from the measured S to give S^g over the full temperature range as shown in Fig. 7. The observed dependence of S^g is approximately T^4.

We have performed detailed numerical calculations of the drag component of both samples, by using Eq. (3) and the standard material parameters for Si.[4] By assuming only screened DP h–p coupling we find $S^g \propto T^{6.3}$ (this is the nominal T^6 dependence noted in Sec.II) for $0.25 < T < 1.5$ K. The results with $\Xi_{DP} = 4.0$ eV are shown in Fig. 6 and 7 as dotted lines. The calculated S^g are approximately correct at 4.2 K, but below 0.5 K they are at least two orders of magnitude too low to explain the experimental values. This behavior is in contrast to that exhibited by a 2D electron gas in a Si-MOSFET where an approximate T^6 dependence was seen for S^g and the calculated magnitude was in good agreement with experiment.[4]

There are two mechanisms that would result in $S^g \propto T^4$ (approximately) both of which have previously been invoked to explain the anomalous behavior of the energy-loss rate. Early data by Xie *et al.*[9] were analyzed in terms of a screened piezoelectric contribution, perhaps arising from the partial ordering of the SiGe alloy (see Ref. 10 for a discussion of

this possibility). Others have suggested that the screening of the DP is ineffective in this system[11,12] which leads to a change in temperature dependence from T^6 to T^4 for S^g, as outlined in Section II. We examine both of these possibilities in detail.

Using an unscreened DP interaction, with coupling constant of $\Xi_{DP} = 2.7$ eV chosen to give the best agreement with experiment, detailed calculations of S^g have been made for the whole temperature range. The results are shown in Figs. 6 and 7 as solid lines for comparison with experiment. The agreement is excellent over the whole temperature range.

Ansaripour *et al.*[11] have found good agreement with experimental energy-loss rate data using an unscreened DP interaction with a coupling constant of $\Xi_{DP} = 3.0$ eV. Leturcq *et al.*[12] have reported that their energy-loss rate data are best represented by the same mechanism with $\Xi_{DP} = 2.8$ eV, together with a small unscreened piezoelectric contribution, this latter appearing only below about 0.5 K. In our case this would correspond to a small term $S^g \propto T^2$ at low temperatures. We do not see such an extra term in the present data, though our precision is relatively low below 0.5 K because of the dominance of S^d in this region. Clearly the agreement between phonon-drag and energy-loss rate results is excellent.

We have also carried out detailed numerical calculations assuming a screened piezoelectric h–p coupling, the magnitude of which was varied to give a reasonable fit to the low temperature data; the value chosen was $h_{14} = 0.6 \times 10^9$ V/m which is 50% the value of that for GaAs. We have also included a screened DP h–p interaction (with $\Xi_{DP} = 4.0$ eV) so that the high temperature data could also be reproduced. Figs. 6 and 7 show the results as dashed lines. In general this model also provides very good agreement with the experiments, though perhaps not quite as good as the unscreened DP at low temperatures.

Neither of the above theoretical models is easily understood from a physical point of view. In the latter, the values used for the piezoelectric coupling constant, h_{14} is uncomfortably high.[12] Still, the fact that phonon drag in Si-MOSFETs[4] and energy loss rates in SiGe electron systems show no piezoelectric coupling[8] would arise naturally with this explanation, since in both of these cases the 2D gas resides in a pure Si channel. In the former model, it is not at all clear why screening should be so ineffective in the SiGe hole system.

It is interesting to compare the present results with that for Si-MOSFETs in more detail. Previous experimental work on Si-MOSFETs at low temperatures has been somewhat contradictory. Phonon drag[4] is consistent with screened DP scattering and no observable piezoelectric component. Energy-relaxation measurements by Fletcher *et al.*[4,26] were incon-

sistent with a screened DP below $\sim$ 1 K, the observed loss rate being considerably larger than predicted. More recent energy-loss rate data[27] have been analyzed by the combination of unscreened DP and unscreened piezoelectric scattering, but the coupling constants were not given. Because phonon-drag and thermopower measure different relaxation rates, momentum in the former case and energy in the latter, the observed discrepancy between the well-behaved drag and the anomalous energy-loss rate in Si-MOSFETs could imply that they are caused by different physical mechanisms. For example, energy-loss rates involving localized excitations would not necessarily be visible in phonon drag. With the SiGe system the two relaxation rates are very consistent, indicating that the same mechanism is responsible for both and is connected with scattering by delocalized excitations, presumably phonons, in both cases.

Regardless of the physical mechanism involved, because S^g involves the momentum relaxation time of the carriers, one can reliably estimate the hole mobility due to phonon scattering, μ_{hp}, in our samples at low temperatures using[6,7]

$$S_i^g = \frac{v_i \Lambda_i}{\mu_{hp,i} T} \tag{9}$$

where v is the sound velocity and the subscript i refers to phonon polarization. Assuming all 3 modes contribute equally to h–p scattering and using an average sound velocity of $\sim$ 5600 m/s, we estimate μ_t/μ_{hp} to be about 10^{-3} for our samples at 4.2 K, and the ratio decreases rapidly with T so that by 1 K it is about 10^{-6}. Clearly, the strong resistivity variation with temperature that is observed in these and similar samples is not related to phonon scattering. Nevertheless, the fact that the fundamental mechanism responsible for the unexpected temperature variation of resistivity is not known leaves open the possibility that h–p scattering might also be affected in some way.

V. CONCLUSIONS

The results show that the magnetic field dependence of both the longitudinal and transverse thermopower are reasonably well understood. The low-field dependences of both the oscillatory and non-oscillatory parts are well described by the Mott model, particularly in the case of the longitudinal thermopower. The transverse thermopower shows some discrepancies, as seems to be typical of this coefficient in 2D systems. On the whole the data agree

with the expectation that drag plays no significant role in either component below about 1 K.

On the other hand the zero field thermopower exhibits various features that are not understood. The data in a magnetic field show that the diffusion component at zero field does not follow the expected linear temperature dependence. This is believed to be connected with the nearby metal-insulator transition, though the detailed mechanism is not known.

The temperature dependence of the phonon-drag contribution at zero field does not correspond to that expected from screened, deformation-potential scattering of holes by phonons. We have investigated two possible models to explain the data, but are unable to decide which, if either, is correct. The first model used an unscreened, deformation-potential, hole-phonon interaction and yielded excellent agreement with experiment. However, it is not clear why screening should be so ineffective in this system. The second model using screened piezoelectric and screened deformation-potential contributions also provides a reasonable representation of the data. The problem with this model is in justifying the magnitude of the large piezoelectric interaction required, and the deformation-potential coupling constant also seems somewhat larger than we would have expected. Both models are consistent with recent work on energy relaxation of holes in a similar system. It is also possible that the metal-insulator transition is playing a role here, though we have no direct evidence to substantiate this.

Acknowledgments

This work is part of a research program of the Stichting voor Fundamenteel Onderzoek der Materie (FOM), financially supported by N.W.O. (The Netherlands). The work was also supported by the Natural Sciences and Engineering Research Council of Canada.

[1] R. Fletcher, Semicond. Sci. Techol. **14**, R1 (1999).

[2] B. Tieke, R. Fletcher, U. Zeitler, M. Henini and J. C. Maan, Phys. Rev. B **58**, 2017 (1998).

[3] R. Fletcher, M. Tsaousidou, P. T. Coleridge, Z. R. Wasilewski and Y. Feng, Physica E **12**, 272 (2002).

[4] R. Fletcher, V. M. Pudalov, Y. Feng, M. Tsaousidou ad P. N. Butcher, Phys. Rev. B**56**, 12422 (1997).

[5] O. A. Mironov, I. G. Gerleman, P. J. Phillps, E. H. C. Parker, M. Tsaousidou and P. N. Butcher, Thin Solid Films **294**, 182 (1997); S. Agan, O. A. Mironov, M. Tsaousidou, T. E. Whall, E. H. C. Parker, P. N. Butcher, Microelectronic Engineering, **51-52**, 527 (2000)

[6] A. Miele, R. Fletcher, E. Zaremba, Y. Feng, C. T. Foxon and J. J. Harris, Phys. Rev. B **58**, 13181 (1998).

[7] M. Tsaousidou, P. N. Butcher and G. P. Triberis, Phys. Rev. B **65**, 165304 (2001).

[8] G. Stoger, G. Brunthaler, G. Bauer, K. Ismail, B. S. Meyerson, J. Lutz and F. Kuchar, Phys. Rev. B **49**, 10417 (1994); Semic. Sci. Technol. **9**, 765 (1994).

[9] Y. H. Xie, R. People, J. C. Bean, K. W. Wecht, Appl. Phys. Lett. **49**, 283 (1986).

[10] G. Braithwaite, N. L. Mattey, E. H. C. Parker, T. E. Whall, G. Brunthaler and G. Bauer, J. Appl. Phys. **81**, 6853 (1997).

[11] G. Ansaripour, G. Braithwaite, M. Myronov, O. A. Mironov, E. H. C. Parker and T. E. Whall, Appl. Phys. Lett. **76**, 1140 (2000).

[12] R. Leturcq, D. L'Hote, R. Tourbot, V. Senz, U. Gennser, T. Ihn, K. Ensslin, G. Dehlinger and D. Grutzmacher, cond-mat/0107457

[13] M. D'Iorio, R. Stoner and R. Fletcher, Solid St. Comm. **65**, 697 (1988).

[14] H. Havlova And L. Smrcka, Phys. Status Solidi (b)**137**, 331 (1986).

[15] R. Fletcher, V. M. Pudalov and S. Cao, Phys. Rev. B **57**, 7174 (1998).

[16] C. Possanzini, R. Fletcher, P. T. Coleridge, Y. Feng, R. L. Williams and J. C. Maan, Phys. Rev. Lett. **90**, 176601 (2003).

[17] T. Ando, A. B. Fowler, and F. Stern, Rev. Mod. Phys. **54**, 437 (1982).

[18] P. J. Price, Ann. Phys. (N.Y.) **133**, 217 (1981).

[19] P. T. Coleridge, R. L. Williams, Y. Feng and P. Zawadzki, Phys. Rev. B **56**, R12764 (1997).

[20] K. Ikeda, R. Fletcher, J. C. Maan and J. Kossut, Phys. Rev. B **65**, 035201 (2002).

[21] S. V. Kravchenko, G. V. Kravchenko, J. E. Furneaux, V. M. Pudalov and M. D'Iorio, Phys. Rev. B **50**, 8039 (1994); S. V. Kravchenko, W. E. Mason, G. E. Bowler, J. E. Furneaux, V. M. Pudalov and M. D'Iorio, Phys. Rev. B **51**, 7038 (1995).

[22] R. Fletcher, V. M. Pudalov, A. D. B. Radcliffe and C. Possanzini, Semicond. Sci. Technol. **16**, 386 (2001).

[23] P. T. Coleridge, R. Stoner and R. Fletcher, Phys. Rev. B **39**, 1120 (1989).

[24] P. T. Coleridge, A. S. Sachrajda, H. Lafontainr and Y. Feng, Phys. Rev. B **54**, 14518 (1996).

[25] V. V. Karavolas and P. N. Butcher, J. Phys.;Condens. Matter **3**, 2597 (1991); X. Zianni and P. N. Butcher, J. Phys.:Condens. Matter **6**, 2713 (1994).

[26] R. Fletcher, V. M. Pudalov, Y. Feng, M. Tsaousidou and P. N. Butcher, Phys. Rev. B**60**, 8392 (1999).

[27] O. Prus, M. Reznikov, U. Sivan and V. Pudalov, Phys. Rev. Lett. **88**, 016801 (2002).

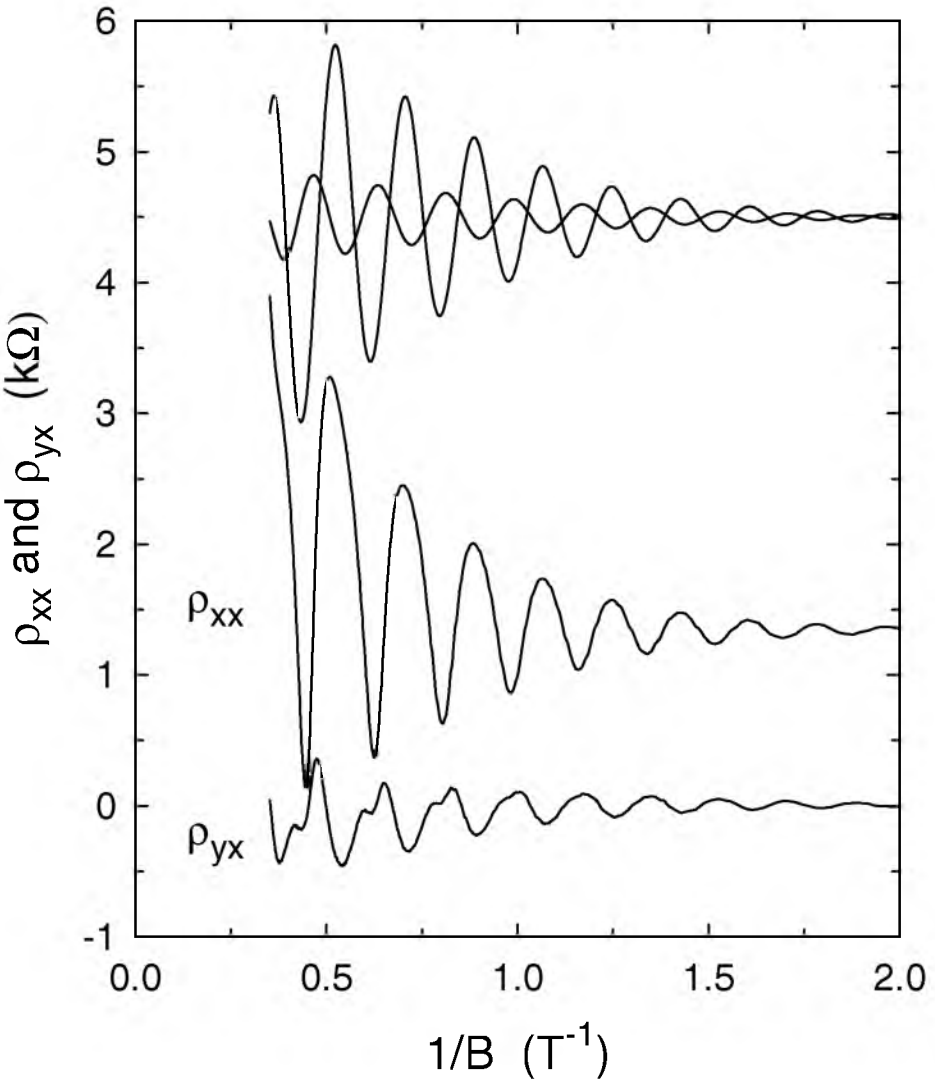

FIG. 1: Experimental data on ρ_{xx} and ρ_{yx} at 0.41 K. The bottom curve is $\tilde{\rho}_{yx}$, obtained by subtracting the part linear in B from the measured ρ_{yx}. The next lowest curve is the measured ρ_{xx}, including the non-oscillatory background. The two superimposed curves at the top (both offset vertically by 4.5 kΩ) are the fundamental harmonic components of the two bottom curves, the larger amplitude curve being $\tilde{\rho}_{xx}$ and the smaller amplitude curve being $\tilde{\rho}_{yx}$. Note the these two curves are in antiphase at low fields, but there is a $\pi/2$ difference at high fields.

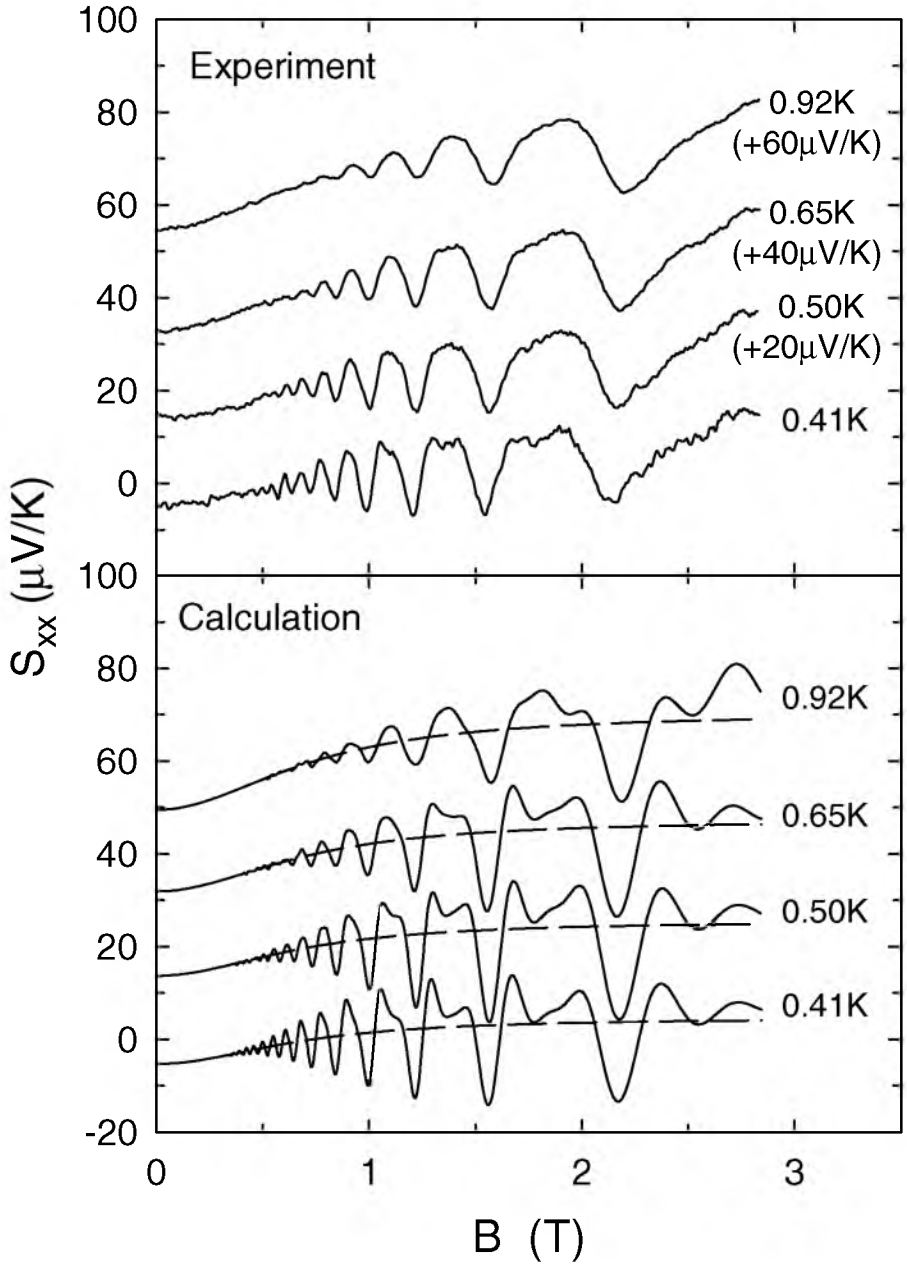

FIG. 2: Measured longitudinal thermopower, S_{xx}, (upper panel) and calculated diffusion component, S^d_{xx}, (lower panel) as a function of magnetic field at various temperatures. The dashed lines in the lower panel are the semi-classical components, $\bar{S}^d_{xx}$. For clarity all but the lowest temperature curves in both panels have been shifted by a vertical offset (as given in brackets in the upper panel).

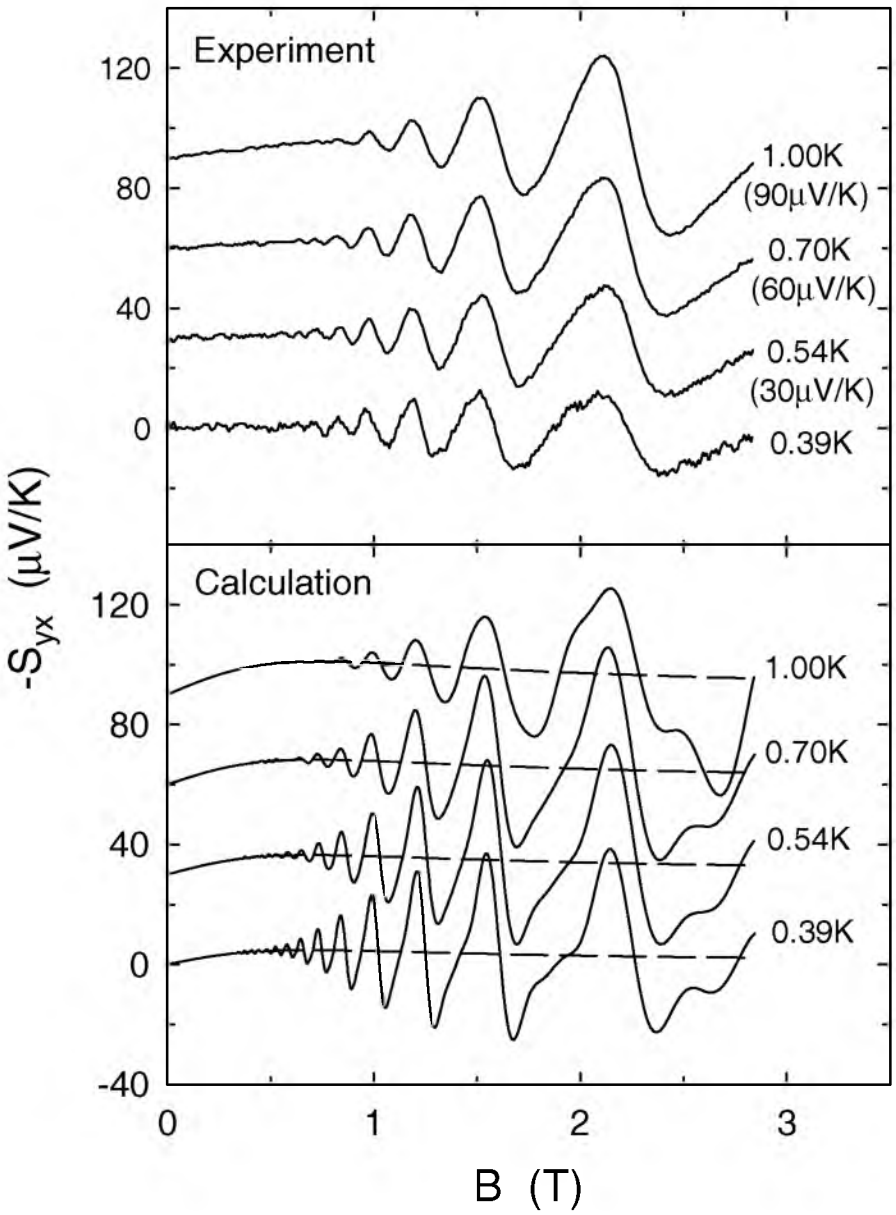

FIG. 3: Measured Nernst-Ettingshausen coefficient, S_{yx}, (upper panel) and calculated diffusion component, S^d_{yx}, (lower panel) as a function of magnetic field at various temperatures. The dashed lines in the lower panel are the semi-classical components, $\bar{S}^d_{yx}$. For clarity all but the lowest temperature curves in both panels have been shifted by a vertical offset (as given in brackets in the upper panel).

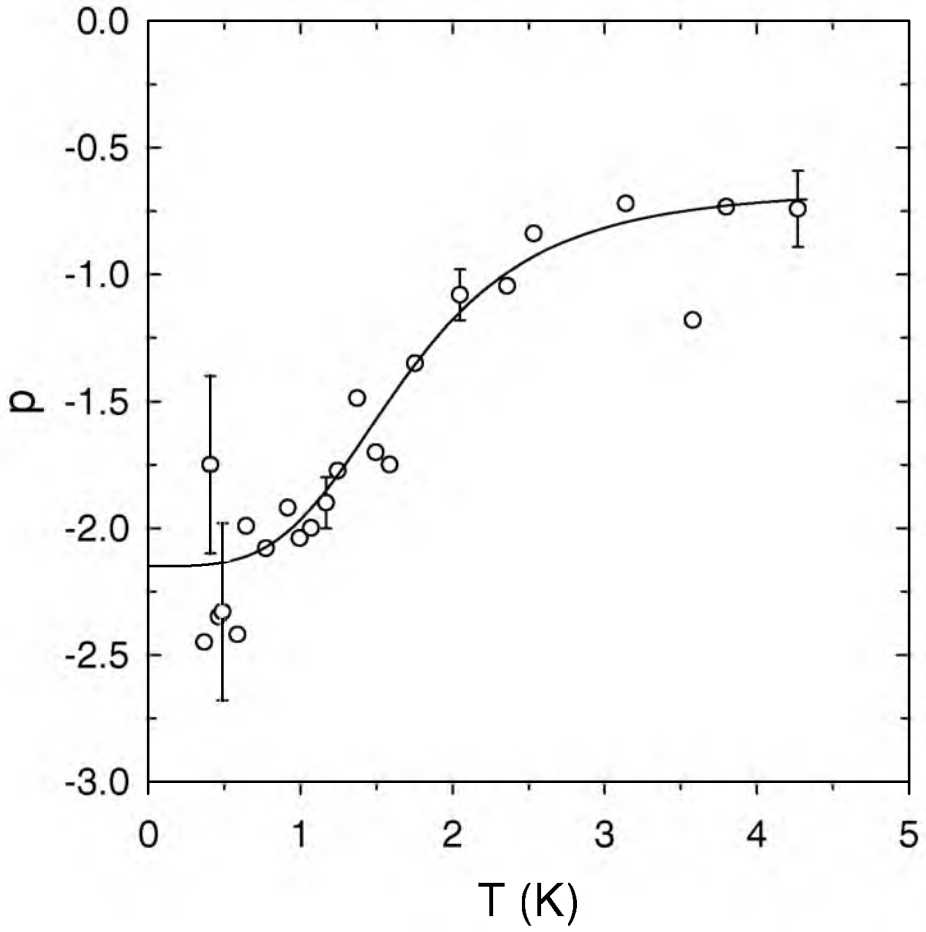

FIG. 4: The circles are the measured coefficient $p = (\partial \ln \tau / \partial \ln E)_{E_F}$ obtained as a fit parameter of the monotonic background of S_{xx} as a function of temperature. The solid line is a phenomenological fit to the experimental data as discussed in the text.

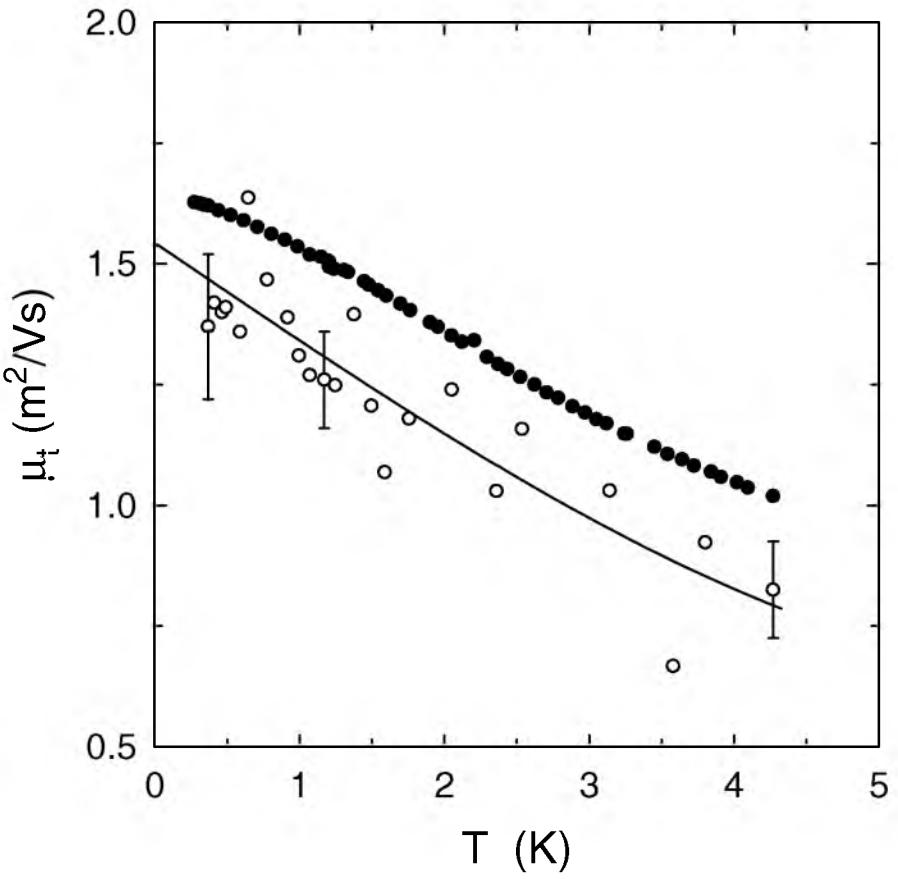

FIG. 5: The open circles are the transport mobility, μ_t, obtained from the magnetic field dependence of the classical background, $\bar{S}_{xx}$, as a function of temperature. The closed symbols are also μ_t but obtained from the resistivity at $B = 0$.

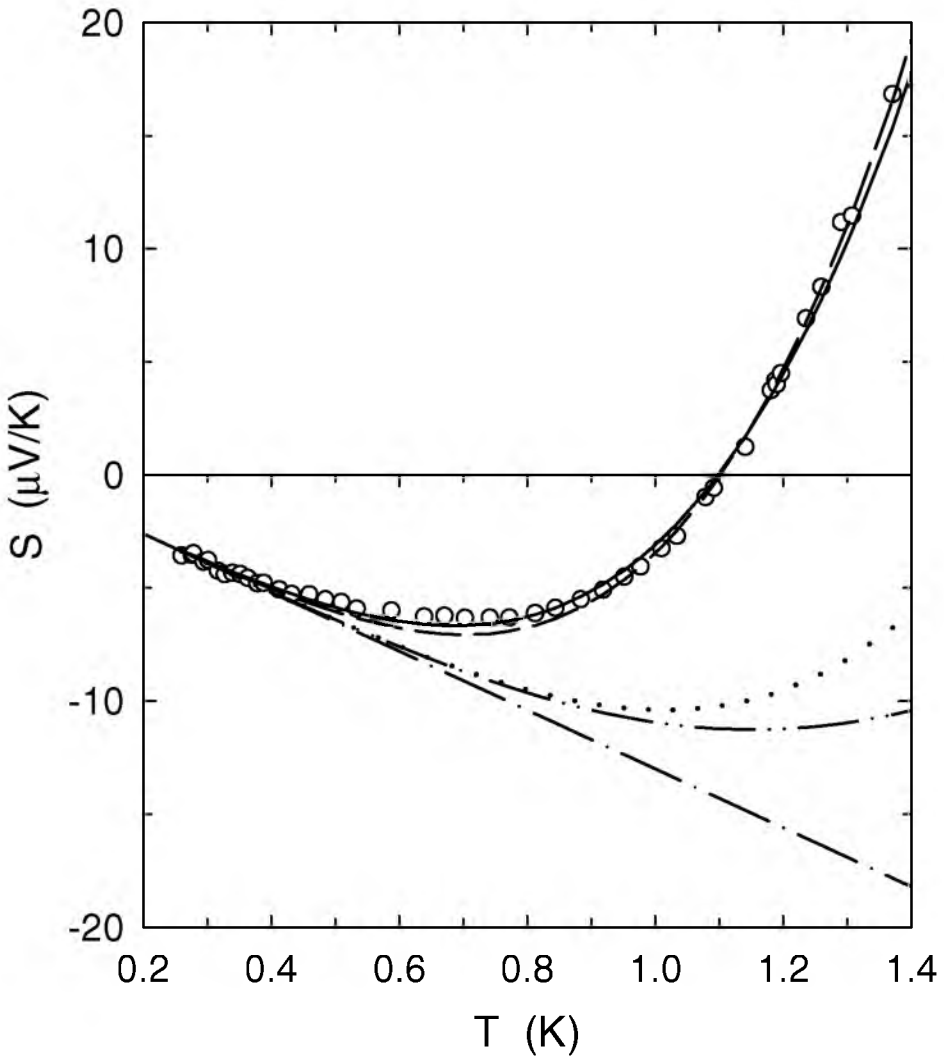

FIG. 6: The circles are the measured thermopower. $-\cdot-$ gives S^d assuming p is constant at -2.21; $-\cdot\cdot-$ gives S^d with p taken from the smooth curve in Fig. 2. The other curves are $S^d + S^g$ with S^d calculated using the smooth curve in Fig. 4 and S^g calculated as follows: — unscreened DP coupling; $\cdots$ screened DP coupling; $---$ screened piezoelectric plus a screened DP coupling.

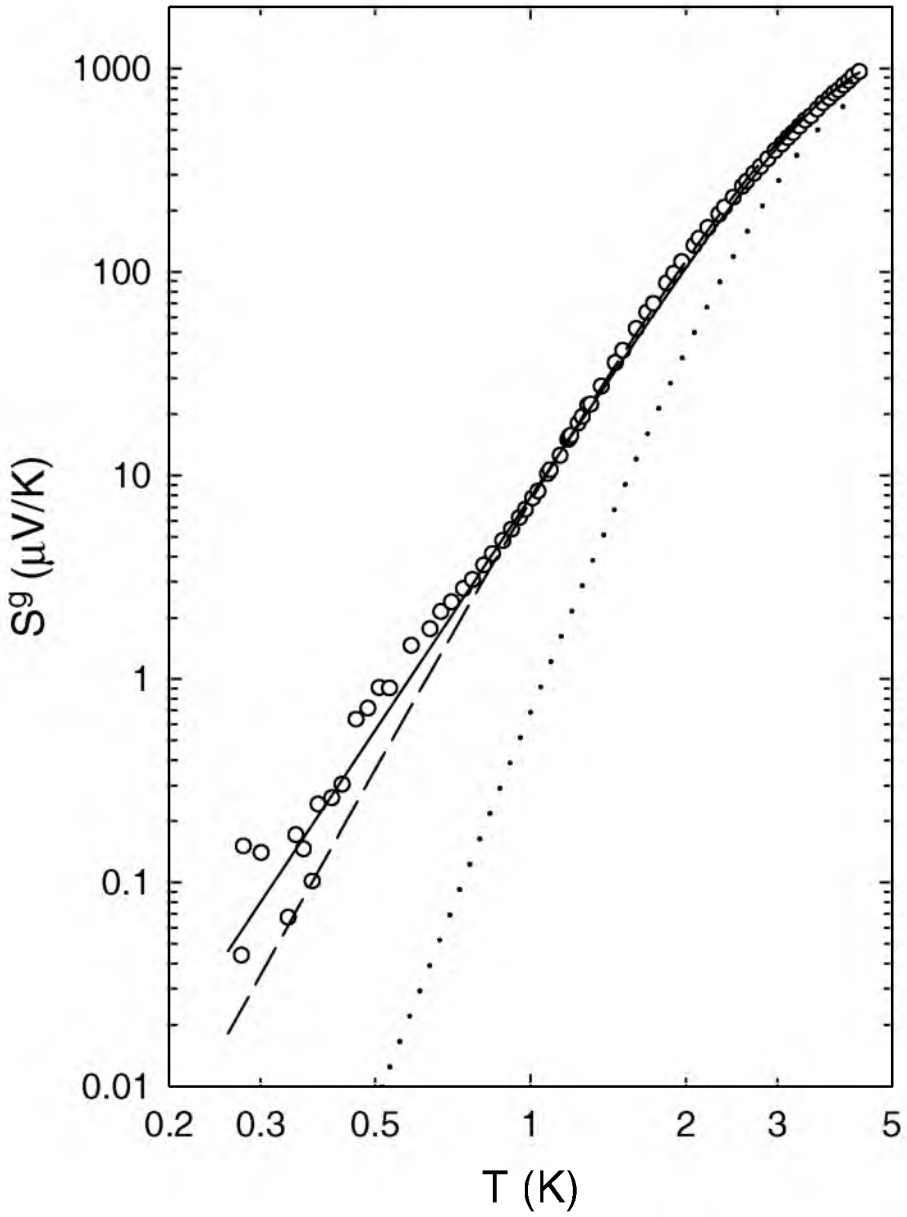

FIG. 7: The circles symbols are the measured phonon-drag thermopower. The various curves are calculations of S^g using the same key as in Fig. 6.